Journal of Photochemistry and Photobiology A: Chemistry 223 (2011) 82–87

Contents lists available at ScienceDirect

Journal of Photochemistry and Photobiology A: Chemistry

journal homepage: www.elsevier.com/locate/jphotochem

# Preparation and characterization of visible-light-driven plasmonic photocatalyst Ag/AgCl/$TiO_2$ nanocomposite thin films

Jiabin Zhou[a,b], Ya Cheng[b], Jiaguo Yu[a,*]

[a] State Key Laboratory of Advanced Technology for Materials Synthesis and Processing, Wuhan University of Technology, 122 Luoshi Road, Wuhan 430070, PR China
[b] School of Resources and Environmental Engineering, Wuhan University of Technology, 122 Luoshi Road, Wuhan 430070, PR China

ARTICLE INFO

*Article history:*
Received 1 February 2011
Received in revised form 3 July 2011
Accepted 27 July 2011
Available online 4 August 2011

*Keywords:*
TiO2 thin films
Ag
AgCl
Plasmonic photocatalysis
Self-stability

ABSTRACT

The Ag/AgCl/$TiO_2$ nanocomposite thin films are prepared on the pre-coated $SiO_2$ soda-lime glass substrates by a sol–gel method for depositing $TiO_2$ films, and then loaded with Ag/AgCl nanoparticles (NPs) by an impregnating precipitation photoreduction method. The as-prepared composite thin film exhibits a highly visible-light photocatalytic activity for degradation of 4-chlorophenol (4-CP) in water. The photocatalytic mechanism is proposed on the basis of the fact that the Ag NPs are photoexcited due to plasmon resonance, and then charge separation is accomplished by the transfer of photoexcited electrons from the Ag NPs to the $TiO_2$ conduction band and the simultaneous formation of $OH^{\bullet}$ radical and $Cl^0$, which cause the photocatalytic degradation of organic pollutants. The proposed mechanism is further confirmed by the detection of hydroxyl radicals. On the other hand, 4-CP can also be oxidized directly by plasmon-induced $h^+$ (or $Ag^+$) on Ag NPs, thereby accelerating the photooxidized Ag NPs back to their initial state. Therefore, the Ag NPs can be rapidly regenerated and the Ag/AgCl/$TiO_2$ system remains self-stability.



## 1. Introduction

In recent ten years, titanium dioxide as one of the most important photocatalytic materials has been extensively investigated due to its wide applications in environmental purification [1–5], photocatalytic water splitting [6–9] and solar energy conversion [10–14], also due to its high photocatalytic activity, good stability, and low cost. However, its limited UV-driven activity largely inhibits its practical application and overall efficiency under natural sunlight, consisting of about 5% UV, 43% visible, and 52% infrared. One of the most potential solutions for enhancing its efficiency is to shift its absorption from the UV region into the visible-light region, allowing for more photons to be absorbed and utilized for decomposing the pollutants. Much progress has been made in the field of visible-light-driven $TiO_2$ by doping metal and nonmetal elements into the $TiO_2$ lattice [14–18], dye photosensitization on the $TiO_2$ surfaces [19], and deposition of noble metals [20–22].

In particular, $TiO_2$ modified by noble metals like Au and Ag has received more and more attention because of its significant increase in the photocatalytic activity of $TiO_2$ [22–24]. Noble metal NPs (Au, Ag) exhibit unique optical properties, owing to the excitation of resonant collective oscillations of the conduction electrons by electromagnetic radiation—the localized surface plasmon resonance (SPR) [25–27]. SPR can dramatically amplify the absorption of visible light and is therefore utilized to develop efficient visible-light-driven plasmonic photocatalysts. For example, Tian and Tatsuma reported plasmon-induced visible-light photoelectrochemistry of gold–$TiO_2$ composite film [26]. Chen et al. also utilized SPR to develop Au/$ZrO_2$ and Au/$SiO_2$ plasmonic photocatalysts with efficient photocatalytic activity under visible-light illumination [28]. In 2008, Wang et al. reported the fabrication of a highly efficient and stable plasmonic photocatalyst Ag/AgCl under visible-light illumination [29]. Very recently, we also reported microwave hydrothermal preparation and visible-light photoactivity of plasmonic photocatalyst Ag–$TiO_2$ nanocomposite hollow spheres [5]. Conventional powdered photocatalysts, however, have an obvious limitation—the need for post-treatment separation in a slurry system after photocatalytic reaction. This can be overcome by immobilizing $TiO_2$ particles as thin films on solid surfaces [30–32].

In this work, new visible-light-driven plasmonic photocatalyst Ag/AgCl/$TiO_2$ nanocomposite thin film were prepared by AgCl NPs deposited on the sol–gel-deposited $TiO_2$ films, and then reducing partial $Ag^+$ ions in the AgCl particles to $Ag^0$ species under xenon lamp irradiation. The prepared samples show high visible-light photocatalytic activity for the photocatalytic degradation of 4-chlorophenol aqueous solution and stability. To the best of our knowledge, this is the first report on the preparation and visible-light photocatalytic activity of plasmonic photocatalyst Ag/AgCl/$TiO_2$ composite thin films prepared by sol–gel and photochemical reduction methods.

* Corresponding author. Tel.: +86 27 87871029; fax: +86 27 87879468.
*E-mail address:* jiaguoyu@yahoo.com (J. Yu).

1010-6030/$ – see front matter © 2011 Elsevier B.V. All rights reserved.
doi:10.1016/j.jphotochem.2011.07.016

## 2. Experimental

### 2.1. Sample preparation

All chemicals used in this study were analytical grade and were purchased from Shanghai Chemical Regent Factory of China without further treatment. Distilled water was used in all experiments. Transparent anatase $TiO_2$ porous nanometer thin films were prepared by the sol–gel dip-coating method [33]. Pre-coated $SiO_2$ soda-lime glass plates (76.2 × 25.4 × 1 mm) were used as the substrates and were carefully cleaned using ultrasonic treatment with base, acid aqueous solution, alcohol, and distilled water, and then dried in an oven at 100 °C. Precursor solutions for $TiO_2$ films were prepared by the following method [33]. Titanium isopropoxide and triethanolamine were dissolved in ethanol. After stirring vigorously for 1 h at room temperature, the mixture of water and ethanol was added dropwise to the solution with a burette under stirring. The resultant alkoxide solution was kept standing at room temperature for hydrolysis reaction for 2 h, resulting in the formation of $TiO_2$ sol. The chemical composition of the starting alkoxide solution was $Ti(OC_3H_7)_4$:$C_2H_5OH$:$H_2O$:$N(C_2H_4OH)_3$ = 1:26.5:1:1 in molar ratio. The cleaned glass plates were used as the substrates for thin films. The substrates coated with $TiO_2$ gel films were heat-treated at 500 °C for 1 h in air in a furnace. The withdrawal speed also was 4 mm/s.

Ag/AgCl NPs were deposited on the as-prepared $TiO_2$ film by an impregnating-precipitation-photoreduction method [34]. Typically, the $TiO_2$ film samples were successively immersed in four different beakers for about 30 min in each beaker. One beaker contained 0.1 M HCl aqueous solution, another contained 0.1 M $AgNO_3$ aqueous solution, and the other two contained distilled water to rinse the excess of each precursor solution from the samples. Such an immersion cycle was repeated several times, typically between 1 and 3 cycles. Finally, the prepared samples were irradiated by a 300 W xenon lamp for 10 min to reduce partial $Ag^+$ ions in the AgCl particles to $Ag^0$ species by photochemical decomposition of AgCl or $TiO_2$ photocatalytic reduction [34].

### 2.2. Characterization

The morphology observation was carried out by an S-4800 field emission scanning electron microscope (SEM, Hitachi, Japan) which was linked with an Oxford Instruments X-ray analysis system at an accelerating voltage of 10 kV. X-ray diffraction (XRD) patterns, obtained on a D/MAX-RB X-ray diffractometer (Rigaku, Japan) using Cu Kα radiation at a scan rate ($2\theta$) of 0.05° $s^{-1}$, were used to determine the identity of any phase present and their crystallite size. The accelerating voltage and applied current were 40 kV and 80 mA, respectively. The average crystallite sizes were calculated according to the Scherrer equation using the full-width half-maximum data after correcting the instrumental broadening. X-ray photoelectron spectroscopy (XPS) measurements were performed on a VG ESCALAB 210 XPS system with Mg Kα (1253.6 eV) source. The spectra were excited by Mg Kα (1253.6 eV) radiation (operated at 200 W) of a twin anode in the constant analyzer energy mode with a pass energy of 30 eV. All the binding energies were referenced to the C1s peak at 284.8 eV of the surface adventitious carbon. UV–vis absorption spectra were obtained on an UV–vis spectrophotometer (UV-2550, Shimadzu, Japan). $BaSO_4$ was used as a reflectance standard.

### 2.3. Photocatalytic activity

The photocatalytic activity of the samples was evaluated by the photocatalytic decomposition of 4-chlorophenol (4-CP) in water at ambient temperature [34], because 4-CP is a kind of hazardous compound and persistent containing-chlorine pollutant [35]. Experiments were as follows: 2.5 × 2.5 $cm^2$ Ag/AgCl/$TiO_2$ film sample was placed in a 15 mL 4-chlorophenol aqueous solution with a concentration of $1 \times 10^{-5}$ M in a rectangle cell (50 W × 50 L × 20 H mm). The solution was allowed to reach an adsorption–desorption equilibrium among the photocatalyst, 4-CP, and water before visible light irradiation. A 300 W xenon lamp through a UV-cutoff filter (≤400 nm), which was positioned 10 cm away from the cell, was used as a visible light source to trigger the photocatalytic reaction. The average light intensity striking on the surface of the reaction solution was about 25 mW $cm^{-2}$. The concentration of 4-CP was determined by an UV–vis spectrophotometer (UV-2550) according to its absorbance at 225 nm. After visible light irradiation for some time (every 10 min), the reaction solution was taken out to measure the concentration change of 4-CP. The visible-light photocatalytic activity of other samples ($TiO_2$ and AgCl/$TiO_2$) was also measured in the same conditions.

### 2.4. Analysis of hydroxyl radical (•OH)

The formation of hydroxyl radicals (•OH) at photo-illuminated samples/water interface was detected by the photoluminescence (PL) method using terephthalic acid as a probe molecule [34]. This method relies on the PL signal at 425 nm of the hydroxylation of terephthalic acid with •OH generated at the water/catalyst interface. The PL intensity of 2-hydroxyterephtalic acid is proportional to the amount of •OH radicals produced in water. The method is rapid, sensitive and specific, needs only a simple standard PL instrumentation. Experimental procedures are similar to the measurement of photocatalytic activity except that 4-CP aqueous solution is replaced by the $5 \times 10^{-4}$ M terephthalic acid aqueous solution with a concentration of $2 \times 10^{-3}$ M NaOH. PL spectra of generated 2-hydroxyterephthalic acid were measured on a Hitachi F-7000 fluorescence spectrophotometer. After visible-light irradiation for every 10 min, the reaction solution was used to measure the increase of the PL intensity at 425 nm excited by 315 nm light.

## 3. Results and discussion

### 3.1. Catalyst characterization

The surface morphology of Ag/AgCl/$TiO_2$ nanocomposite thin film was observed by SEM. Fig. 1a presents a SEM image of the $TiO_2$ thin films, which shows homogeneous, smooth coating with regularly arranged granular microstructure and flat texture. A cross-sectional view (not shown here) of the film indicates that the film thickness is about 100 nm. Fig. 1b shows the SEM images of Ag/AgCl nanoparticles deposited on the $TiO_2$ thin films. It can be observed some dotted sphere particles with a size range of from 10 to 50 nm are uniformly deposited on the surface of $TiO_2$ films, indicating the increase of the surface roughness of the thin films. This implies that the specific surface area of Ag/AgCl/$TiO_2$ nanocomposite thin films is larger than that of pure $TiO_2$ thin films and the light absorption of the composite thin films is enhanced due to the enhanced light scattering. The composition of the composite film was determined by energy dispersive X-ray spectroscopy (EDX) experiments, which were carried out in the SEM. The EDX result shows that the sample contains Ti, O, Si, Ag and Cl elements (not shown here). Ti and O peaks result from $TiO_2$ film and Si peak is from glass substrate. Ag and Cl elements are from the deposited AgCl and reduced Ag particles.

To get further information about the phase structure of the composite thin film, the samples were investigated by XRD. Fig. 2 shows

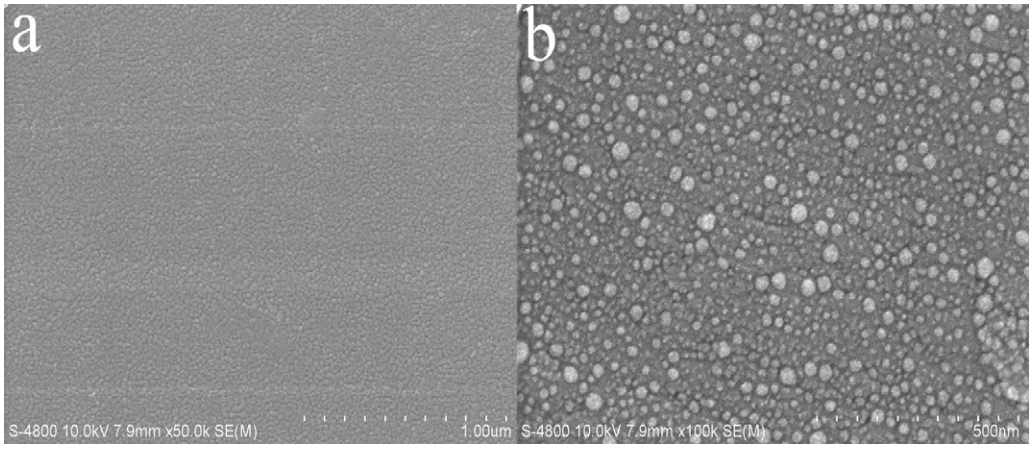


**Fig. 1.** SEM images of $TiO_2$ (a) and Ag/AgCl/$TiO_2$ nanocomposite (b) thin films.

XRD pattern of the nanocomposite thin film sample. Quantitative analysis of this pattern indicates that all peaks in the pattern can be indexed using the anatase phase of $TiO_2$ (JCPDS file No: 21-1272), the cubic phase of AgCl with lattice constant $a = 5.5491$ Å (JCPDS file No: 31-1238) and metallic Ag (JCPDS file No: 65-2871), which are marked with A, C and S in Fig. 2, respectively. The diffraction peaks of anatase phase are from the $TiO_2$ thin film. The average crystallite size of the $TiO_2$ films is 12.6 nm, determined by Scherrer's equation using the main (1 0 1) diffraction peak. The sharp diffraction peaks of AgCl suggest that the deposited the AgCl NPs are well crystallized. The average crystalline size is calculated to be 20.5 nm, which is consistent with the corresponding SEM observations. The metallic Ag is from the photochemical or photocatalytic reduction decomposition of AgCl under Xenon lamp light irradiation in the presence of $TiO_2$. Therefore, it is not too surprising that the sample contains a small amount of metallic silver (ca. 3.8 nm) coexisting with AgCl [34].

Fig. 3 shows a comparison of UV/visible spectra of the $TiO_2$, AgCl/$TiO_2$ and Ag/AgCl/$TiO_2$ samples. For all the samples, the absorption peaks at the wavelength shorter than 390 nm is due to the intrinsic bandgap absorption of anatase $TiO_2$. It is worth mentioning that the $TiO_2$ thin films loaded with Ag/AgCl exhibit a strong adsorption peak in visible light region. This is ascribed to the existence of Ag NPs produced by photochemical decomposition of AgCl, and thus the incident photon frequency is resonant with the collective excitation of conduction electrons of the Ag NPs, called the localized surface plasmon resonance (LSPR) [5,27,34].

The elemental compositions and chemical status of the thin films were further analyzed by XPS. The photoelectron peaks for Ti 2p and O 1s appear clearly at binding energy $E_b$ of 458 and 531 eV, respectively (Fig. 4A). The XPS peak for C 1s at $E_b = 284.8$ eV is due to the adventitious hydrocarbon from the XPS instrument itself. Si 2p peak at $E_b = 103.0$ eV is from glass substrate. Ag (368 eV) and Cl peaks (199 eV) are from the deposited Ag/AgCl particles on the thin films. Fig. 4B shows the high resolution XPS spectra of the O 1s for the thin films. The O 1s region is decomposed into three peaks. The main contribution is attributed to Ti–O in $TiO_2$, and the other two kinds of oxygen contributions can be ascribed to the OH in Ti–OH and the C–O in residual organic compounds, respectively. The thin films easily adsorb water vapor in air, leading to the formation of hydroxyl on the films. The high hydroxyl density on the surface of the thin films would be beneficial in charge transfer and thus enhance the photocatalytic activity.

### 3.2. Photocatalytic activity

For pure $TiO_2$ thin films, no visible-light photocatalytic activity is observed because they are not excited by visible light. Furthermore, AgCl/$TiO_2$ thin films show weak visible-light photocatalytic activity due to large indirect band gap of AgCl (3.25 eV) and $TiO_2$ (3.2 eV). Under UV light irradiation, Grains of AgCl are photosensitive to UV light due to their point ionic defects and electron traps [29], which led to a small amount of metallic Ag deposited on the

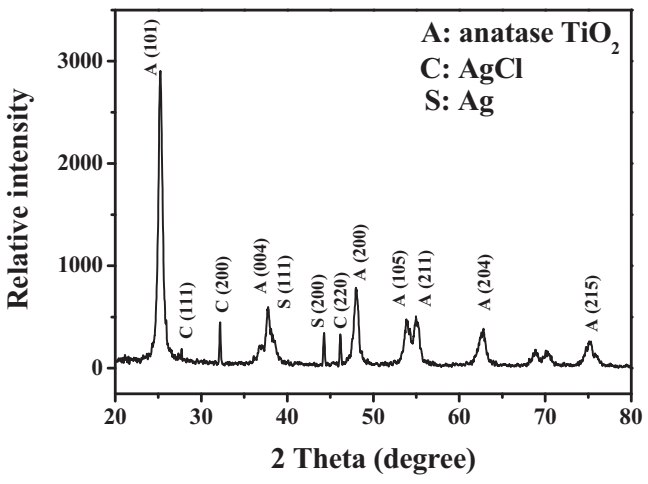


**Fig. 2.** XRD pattern of Ag/AgCl/$TiO_2$ nanocomposite thin film.

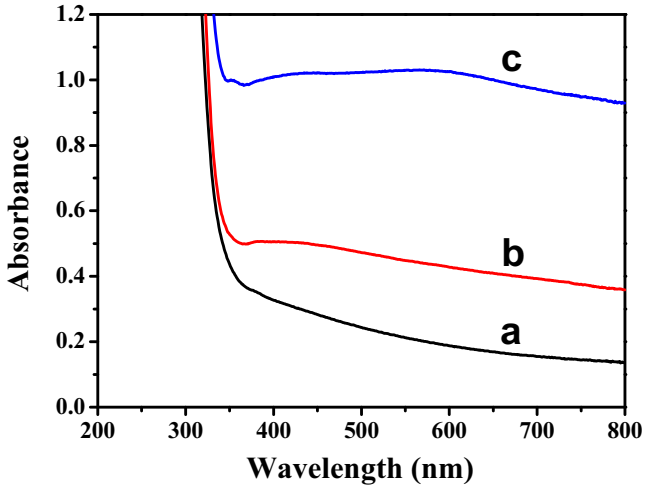


**Fig. 3.** UV–vis spectra of $TiO_2$ (a), AgCl/$TiO_2$ (b), and Ag/AgCl/$TiO_2$ (c) thin films.

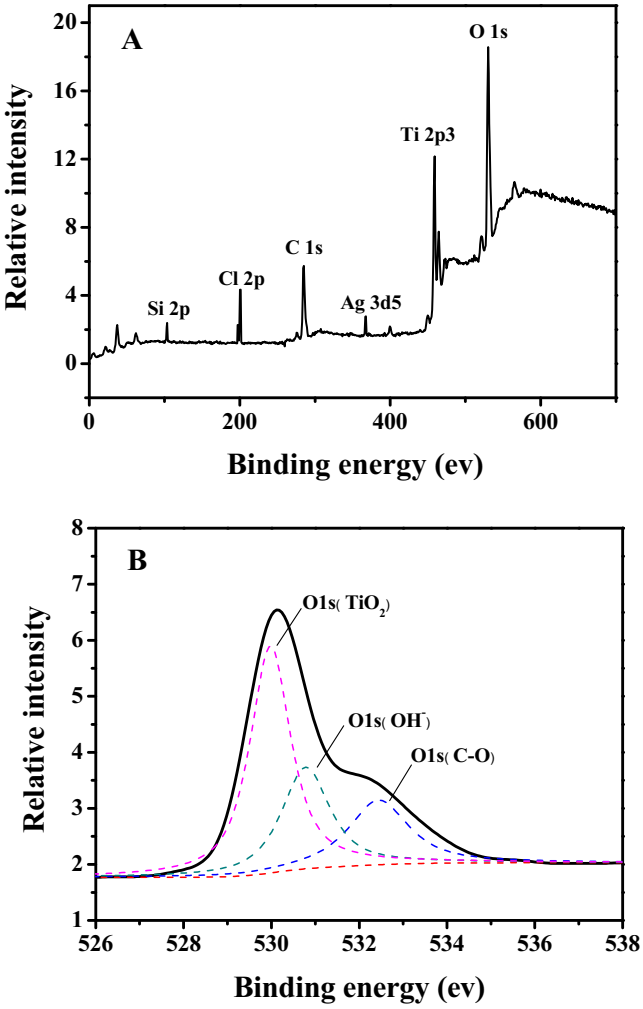


**Fig. 4.** XPS survey spectra (A) of Ag/AgCl/$TiO_2$ nanocomposite thin films and corresponding high-resolution XPS spectra (B) of O 1s region.

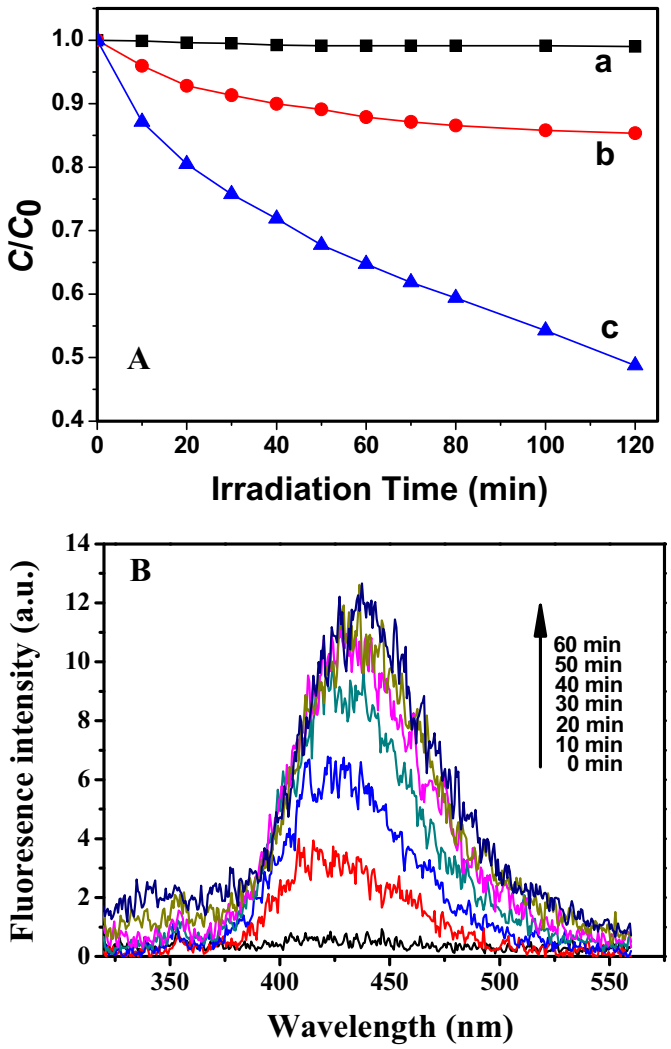


**Fig. 5.** (A) Comparison of photocatalytic activity of $TiO_2$ (a), AgCl/$TiO_2$ (b), and Ag/AgCl/$TiO_2$ (c) thin films, and (B) PL spectral changes with visible-light irradiation time for the Ag/AgCl/$TiO_2$ nanocomposite thin films.

surface of AgCl particle. The prepared Ag/AgCl/$TiO_2$ nanocomposite thin films exhibit obvious visible-light photocatalytic activity (as shown in Fig. 5A). With increasing irradiation time, the concentration of 4-CP decrease steadily, and about half of the target compound was decomposed within 120 min. We found that other organic pollutants such as rhodamine B, methylene blue, and phenol can also be decomposed by the prepared composite films under visible-light irradiation, indicating that the prepared Ag/AgCl/$TiO_2$ film is an efficient visible-light photocatalyst. As a photocatalyst, its stability is very important for its practical application. The stability of plasmonic photocatalyst Ag/AgCl/$TiO_2$ film is further investigated by the recycle experiments of photocatalyst. After 5 recycles for the photodegradation of 4-CP, the catalyst does not exhibit any significant loss of activity (not shown here), indicating that the catalysts are relative stable during the photocatalytic oxidation of the pollutant molecules.

### 3.3. Photocatalytic mechanism

The photocatalytic activity and stability of the Ag/AgCl/$TiO_2$ nanocomposite thin films can be understood by the following proposed mechanism (as shown in Fig. 6), which is similar to our recently proposed mechanism of plasmonic photocatalysis [5,34]. Under visible-light irradiation, photo-generated electron–hole pairs are formed in Ag nanoparticles due to surface plasmon resonance. The photoexcited electrons at the silver nanoparticles are injected into the conduction band of $TiO_2$. Why can the photoexcited electrons at the silver nanoparticles inject into the $TiO_2$ conduction band? This is due to the fact that before visible light irradiation, the Fermi level of $TiO_2$ and Ag NPs is the same. Under visible light irradiation, $TiO_2$ cannot be excited and its Fermi level keeps un-change. On the contrary, Ag NPs can absorb visible light due to its SPR absorption, which results in the up shift of Fermi level of Ag NPs. Therefore, the photoexcited electrons at the silver NPs can be easily injected into the conduction band of $TiO_2$. Then, the injected electrons can be transferred to the adsorbed $O_2$, firstly producing superoxide radical anions, $O_2^{-\bullet}$, then on protonation yields HOO$^\bullet$ radicals. The HOO$^\bullet$ radicals and the trapped electrons combine to produce $H_2O_2$, finally forming $^\bullet$OH radicals. These $^\bullet$OH active species can cause the degradation and mineralization of 4-CP. Nevertheless, the left holes can transfer to the AgCl surface due to the negative surface charge [34], which could cause the oxidation of $Cl^-$ ions to $Cl^0$ atoms [29,34,36]. Because of the high oxidation ability of the chlorine atoms, the 4-CP could be oxidized by the chlorine atoms and hence the $Cl^0$ could be reduced to chloride ions again. So the Ag/AgCl composite could remain stable without deterioration [29,34,36]. The detailed reactions are described by Eqs. (1–9) as follows [5,34,37]:

$$\text{Ag-NPs} + h\nu(\text{visible}) \rightarrow \text{Ag-NPs}^* \quad (1)$$

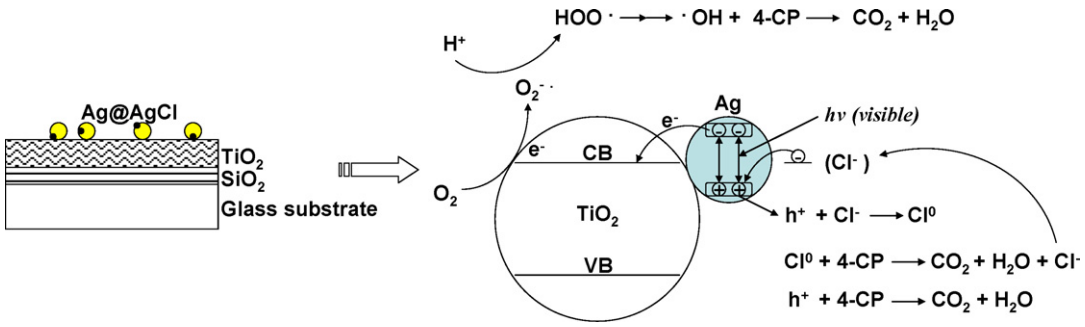


**Fig. 6.** Sample configurations and schematic diagram for the charge separation and transfer at visible-light irradiated Ag/AgCl/$TiO_2$ nanocomposite thin films.

$$\text{Ag-NPs}^* + \text{TiO}_2 \rightarrow \text{Ag-NPs}^{+\bullet}(h^+) + \text{TiO}_2(e^-) \quad (2)$$

$$\text{TiO}_2(e^-) + \text{O}_2 \rightarrow \text{TiO}_2 + \text{O}_2^{-\bullet} \quad (3)$$

$$\text{O}_2^{-\bullet} + \text{H}^+ \rightarrow \text{HOO}^\bullet \quad (4)$$

$$e^- + \text{HOO}^\bullet + \text{H}^+ \rightarrow \text{H}_2\text{O}_2 \quad (5)$$

$$\text{H}_2\text{O}_2 + e^- \rightarrow \bullet\text{OH} + \text{OH}^- \quad (6)$$

$$\text{4-CP} + {}^\bullet\text{OH} \rightarrow \text{CO}_2 + \text{H}_2\text{O} + \text{Cl}^- \quad (7)$$

$$\text{Ag-NPs}^{+\bullet}(h^+) + \text{Cl}^- \rightarrow \text{Ag-NPs} + \text{Cl}^0 \quad (8)$$

$$\text{4-CP} + \text{Cl}^0(\text{or } h^+) \rightarrow \text{CO}_2 + \text{H}_2\text{O} + \text{Cl}^- \quad (9)$$

The proposed mechanism was further confirmed by the detection of •OH. It can be seen from Fig. 5B that a gradual increase in PL intensity at 425 nm is observed with increasing irradiation time. On the contrary, no PL is observed in the absence of visible-light irradiation or Ag/AgCl/$TiO_2$ nanocomposite thin film sample. This implies that the fluorescence is from the chemical reactions between terephthalic acid and •OH formed during photocatalytic reactions [5,34,38]. Further experiments show that no PL signals are observed for the $TiO_2$ thin films sample (not shown here) because pure $TiO_2$ are not activated by visible light, implying no visible-light photocatalytic activity for the pure $TiO_2$ sample. Therefore, the hydroxyl radical experiments further confirmed that hydroxyl radical is one of active species and indeed participates in photocatalytic degradation of the organic pollutants. It should be noted that on the one hand, the produced $OH^\bullet$ radicals and $Cl^0$ can cause the degradation and mineralization of 4-CP, on the other hand, 4-CP can also be oxidized directly by plasmon-induced $h^+$ (or $Ag^+$) on Ag NPs, thereby accelerating the photooxidized Ag NPs back to their initial state. This was confirmed by many published results [34,39–42]. Therefore, the Ag NPs can be rapidly regenerated and the Ag/AgCl/$TiO_2$ system remains self-stability. Added experiments also indicated that $Ag^+$ can cause the degradation of 4-chlorophenol aqueous solution under visible-light irradiation.

## 4. Conclusions

Visible-light-driven plasmonic photoctalyst Ag/AgCl/$TiO_2$ nanocomposite thin films are successfully prepared by AgCl NPs deposited on $TiO_2$ thin films followed by reducing partial $Ag^+$ ions of the AgCl particles to $Ag^0$ species under UV irradiation. The resulting plasmonic photoctalyst exhibits an obviously visible-light photocatalytic activity for photocatalytic degradation of 4-CP aqueous solution. This can be understood by the proposed mechanism. Under visible-light irradiation, the photoexcited electrons at the silver NPs are injected into the conduction band of $TiO_2$. Then, the injected electrons can be transferred to the adsorbed $O_2$, firstly producing superoxide radical anions, $O_2^{-\bullet}$, then $HOO^\bullet$ radicals, $H_2O_2$, finally forming $OH^\bullet$ radicals, which cause the degradation and mineralization of 4-CP. On the other hand, 4-CP can also be oxidized directly by plasmon-induced $h^+$ (or $Ag^+$) on Ag NPs, thereby accelerating the photooxidized Ag NPs back to their initial state. Therefore, the Ag NPs can be rapidly regenerated and the Ag/AgCl/$TiO_2$ system remains self-stability.

## Acknowledgements

This work was partially supported by the National Natural Science Foundation of China (20877061 and 51072154), Natural Science Foundation of Hubei Province (2010CDA078), China Postdoctoral Science Foundation project (20090460998), National Basic Research Program of China (2007CB613302) and Self-determined and Innovative Research Funds of SKLWUT.

## References

[1] A. Fujishima, T.N. Rao, D.N. Tryk, J. Photochem. Photobiol. 1 (2000) 1.
[2] M.R. Hoffmann, S.T. Martin, W. Choi, D.W. Bahnemann, Chem. Rev. 95 (1995) 69.
[3] H. Park, W. Choi, J. Phys. Chem. B 108 (2004) 4086.
[4] M. Ksibi, S. Rossignol, J.M. Tatibouet, C. Trapalis, Mater. Lett. 62 (2008) 4204.
[5] Q.J. Xiang, J.G. Yu, B. Cheng, H.C. Ong, Chem. Asian J. 5 (2010) 1466.
[6] Y.X. Li, Y.Z. Xie, S.Q. Peng, G.X. Lu, S.B. Li, Chemosphere 63 (2006) 1312.
[7] Y.X. Li, G.X. Lu, S.B. Li, J. Photochem. Photobiol. A 152 (2002) 219.
[8] J.G. Yu, L.F. Qi, M. Jaroniec, J. Phys. Chem. C 114 (2010) 13118.
[9] J.G. Yu, J. Zhang, M. Jaroniec, Green Chem. 12 (2010) 1611.
[10] B. O'Regan, M. Gratzel, Nature 353 (1991) 737.
[11] L. Zhao, J.G. Yu, J.J. Fan, P.C. Zhai, S.M. Wang, Electrochem. Commun. 11 (2009) 2052.
[12] J.G. Yu, J.J. Fan, L. Zhao, Electrochim. Acta 55 (2010) 597.
[13] A. Hagfeldt, M. Gratzel, Chem. Rev. 95 (1995) 49.
[14] J.G. Yu, J.J. Fan, K.L. Lv, Nanoscale 2 (2010) 2144.
[15] R. Asahi, T. Morikawa, T. Ohwaki, K. Aoki, Y. Taga, Science 293 (2001) 269.
[16] H. Irie, Y. Watanabe, K. Hashimoto, J. Phys. Chem. B 107 (2003) 5483.
[17] S. Liu, J. Yu, W. Wang, Phys. Chem. Chem. Phys. 12 (2010) 12308.
[18] J.G. Yu, Q.J. Xiang, M.H. Zhou, Appl. Catal., B 90 (2009) 595.
[19] S.G. Hickey, D.J. Riley, E.J. Tull, J. Phys. Chem. B 104 (2000) 7623.
[20] J.G. Yu, L. Yue, S.W. Liu, B.B. Huang, X.Y. Zhang, J. Colloid Interface Sci. 334 (2009) 58.
[21] R. Priya, K.V. Baiju, S. Shukla, S. Biju, M.L.P. Reddy, K. Patil, K.G.K. Warrier, J. Phys. Chem. C 113 (2009) 6243.
[22] J.X. Li, J.H. Xu, W.L. Dai, K.N. Fan, J. Phys. Chem. C 113 (2009) 8343.
[23] H.M. Sung-Suh, J.R. Choi, H.J. Hah, S.M. Koo, Y.C. Bae, J. Photochem. Photobiol. A 163 (2004) 37.
[24] J.G. Yu, J.F. Xiong, B. Cheng, S.W. Liu, Appl. Catal., B 60 (2005) 211.
[25] K. Awazu, M. Fujimaki, C. Rockstuhl, J. Tominaga, H. Murakami, Y. Ohki, N. Yoshida, T. Watanabe, J. Am. Chem. Soc. 130 (2008) 1676.
[26] Y. Tian, T. Tatsuma, J. Am. Chem. Soc. 127 (2005) 7632.
[27] J. Yu, H. Tao, B. Cheng, Chemphyschem. 11 (2010) 1617.
[28] X. Chen, H.Y. Zhu, J.C. Zhao, Z.T. Zheng, X.P. Gao, Angew. Chem. Int. Ed. 27 (2008) 5353.
[29] P. Wang, B.B. Huang, X.Y. Qin, X.Y. Zhang, Y. Dai, J.Y. Wei, M.H. Whangbo, Angew. Chem. Int. Ed. 47 (2008) 7931.
[30] G. Zhao, H. Kozuka, T. Yoko, Thin Solid Films 277 (1996) 147.
[31] J.G. Yu, H.G. Yu, B. Cheng, X.J. Zhao, J.C. Yu, W.K. Ho, J. Phys. Chem. B 107 (2003) 13871.
[32] S. Deki, Y. Aoi, O. Hiroi, A. Kajinami, Chem. Lett. 6 (1996) 433.
[33] J.C. Yu, J. Yu, J. Zhao, Appl. Catal., B 36 (2002) 31.
[34] J.G. Yu, G.P. Dai, B.B. Huang, J. Phys. Chem. C 113 (2009) 16394.

[35] O. Botalova, J. Schwarzbauer, T. Frauenrath, L. Dsikowitzky, Water Res. 43 (2009) 3797.
[36] H. Xu, H.M. Li, J. Xia, S. Yin, Z. Luo, L. Liu, L. Xu, ACS Appl. Mater. Interface 3 (2011) 22.
[37] T. Wu, G. Liu, J. Zhao, H. Hidaka, N. Serpone, J. Phys. Chem. B 102 (1998) 5845.
[38] Q. Xiang, J. Yu, P.K. Wong, J. Colloid Interface Sci. 357 (2011) 163.
[39] C. Hu, T.W. Peng, X.X. Hu, Y.L. Nie, X.F. Zhou, J.H. Qu, H. He, J. Am. Chem. Soc. 132 (2010) 857.
[40] X.F. Wang, S.F. Li, H.G. Yu, J.G. Yu, S.W. Liu, Chem. Eur. J. 17 (2011) 7777.
[41] X.F. Wang, S.F. Li, Y.Q. Ma, H.G. Yu, J.G. Yu, J. Phys. Chem. C 115 (2011) 14648.
[42] C.H. An, S. Peng, Y.G. Sun, Adv. Mater. 22 (2010) 2570.